Published in final edited form as:
Exp Neurol. 2013 September ; 247: 653–662. doi:10.1016/j.expneurol.2013.03.001.

Three-dimensional evaluation of retinal ganglion cell axon regeneration and pathfinding in whole mouse tissue after injury

Xueting Luo[a], **Yadira Salgueiro**[a], **Samuel R. Beckerman**[a], **Vance P. Lemmon**[a], **Pantelis Tsoulfas**[a], and **Kevin K. Park**[a]

Xueting Luo: Xluo@med.miami.edu; Yadira Salgueiro: Ysalgueiro@med.miami.edu; Samuel R. Beckerman: Sbeckerman@med.miami.edu; Vance P. Lemmon: Vlemmon@med.miami.edu; Pantelis Tsoulfas: Ptsoulfa@med.miami.edu; Kevin K. Park: Kpark@med.miami.edu

[a]Miami Project to Cure Paralysis and Department of Neurosurgery, University of Miami, Miller School of Medicine, Miami, FL, 33136, USA.

Abstract

Injured retinal ganglion cell (RGCs) axons do not regenerate spontaneously, causing loss of vision in glaucoma and after trauma. Recent studies have identified several strategies that induce long distance regeneration in the optic nerve. Thus, a pressing question now is whether regenerating RGC axons can find their appropriate targets. Traditional methods of assessing RGC axon regeneration use histological sectioning. However, tissue sections provide fragmentary information about axonal trajectory and termination. To unequivocally evaluate regenerating RGC axons, here we apply tissue clearance and light sheet fluorescence microscopy (LSFM) to image whole optic nerve and brain without physical sectioning. In mice with PTEN/SOCS3 deletion, a condition known to promote robust regeneration, axon growth followed tortuous paths through the optic nerve, with many axons reversing course and extending toward the eye. Such aberrant growth was prevalent in the proximal region of the optic nerve where strong astroglial activation is present. In the optic chiasms of PTEN/SOCS3 deletion mice and PTEN deletion/Zymosan/cAMP mice, many axons project to the opposite optic nerve or to the ipsilateral optic tract. Following bilateral optic nerve crush, similar divergent trajectory is seen at the optic chiasm compared to unilateral crush. Centrally, axonal projection is limited predominantly to the hypothalamus. Together, we demonstrate the applicability of LSFM for comprehensive assessment of optic nerve regeneration, providing in-depth analysis of the axonal trajectory and pathfinding. Our study indicates significant axon misguidance in the optic nerve and brain, and underscores the need for investigation of axon guidance mechanisms during optic nerve regeneration in adults.

Keywords

PTEN; SOCS3; axon regeneration; axon growth; retinal ganglion cell; axotomy

Corresponding Author: Kevin K. Park, Miami Project to Cure Paralysis, University of Miami, Miller School of Medicine, Miami, FL, 33136, USA. Phone: (1) 305 243 2493, Email Address: kpark@med.miami.edu.

INTRODUCTION

Retinal ganglion cells (RGC) do not regenerate their axons, leading to loss of visual functions in glaucoma and after trauma or stroke. Studies on the limited regenerative capacity of RGCs have identified several strategies that stimulate axon regeneration. These include enhancing the intrinsic growth capacity as well as neutralizing repulsive cues in the environment (Cho et al, 2005; Duffy et al, 2012; Leaver et al, 2006; Lingor et al, 2008; Liu et al, 2006; Muller et al, 2007; Qiu et al, 2002; Su et al, 2008; Winzeler et al, 2011; Wong et al, 2003). We and others have used knockout (KO) mice to demonstrate that RGC-specific deletion of PTEN (phosphatase and tensin homolog), SOCS3 (suppressor of cytokine signaling 3) or KLF4 (Krüppel like factor 4) induces RGC axon regeneration (Moore et al, 2009; Park et al, 2008; Smith et al, 2009). More recent studies have shown that combining PTEN KO mice with either SOCS3 deletion, or Zymosan and a cAMP analogue leads to substantially more regeneration than targeting them individually (de Lima et al, 2012; Kurimoto et al, 2010; Sun et al, 2011), pointing to the importance of targeting multiple factors to induce extensive regeneration.

With the recent progress made in promoting RGC axon regeneration, it is becoming increasingly important to investigate whether regenerating RGC axons can find their targets in the brain. While appropriate pathfinding of RGC axons has been documented comprehensively in regeneration-competent species including fish and amphibians (Beazley et al, 1997; Becker & Becker, 2007; Stelzner et al, 1986), the degree to which RGC axons in adult mammals correctly reinnervate their targets is unclear.

A common method for assessing optic nerve regeneration is histological sectioning. However, tissue sections provide incomplete spatial information. For instance, it is difficult to determine the precise trajectory of axons or their final destinations. In this study, we applied a tetrahydrofuran (THF) based-clearing method that renders tissues relatively transparent (Becker et al, 2012; Erturk et al, 2012), and combined it with LSFM, allowing deep tissue fluorescence imaging in unsectioned optic nerve and brain. Using these methods, we found in PTEN/SOCS3 KO mice that regenerating axons follow circuitous paths, with many axons making multiple turns and extending back to the eye. Axon turning was prevalent in nerve regions with strong astroglial activation. Many RGC axons generated branches in the optic nerve and brain as they re-grow. In the optic chiasm, a major decision point en route to visual targets, high numbers of regenerating axons in PTEN/SOCS3 KO mice or PTEN KO/Zymosan/cAMP analogue-treated mice diverge into the ipsilateral optic tract or to the opposite optic nerve. Following bilateral optic nerve crush, a similar growth pattern is seen at the optic chiasm compared to unilateral crush. Centrally, axonal projection is limited primarily to the hypothalamus. In summary, we demonstrated the combined application of tissue clearance and LSFM for comprehensive analysis of optic nerve regeneration, providing in-depth assessment of the axonal trajectory. Our study shows substantial misdirection of RGC axon growth in adult mice, and underscores the need for investigation into the mechanisms that underlie misguidance during regeneration in adults.

MATERIALS AND METHODS

All experimental procedures were performed in compliance with animal protocols approved by the IACUC at the University of Miami Miller School of Medicine. For all surgical procedures, mice were anaesthetized with ketamine and xylazine. Eye ointment containing atropine sulphate was applied preoperatively to protect the cornea during surgery, and Buprenorphine (0.05mg/kg, Bedford Lab) was administrated as post-operative analgesic.

Mice, optic nerve crush injury and intravitreal injection

SOCS3$^{f/f}$/PTEN$^{f/f}$ (Sun et al, 2011) mice (female; 4–6 weeks old) were intravitreally injected with 1–2 μl volume of AAV2-Cre in the left eyes at 2 weeks prior to crush injury. 1 μl (1 μg/μl) ciliary neurotrophic factor (CNTF; Pepro Tech) was intravitreally injected immediately after injury and at 3 days post-injury, and biweekly thereafter. PTEN KO/ZYM/cAMP mice, PTEN$^{f/f}$ (Groszer et al, 2001) (female; 8 weeks old) received intravitreal AAV2-Cre injection followed by optic nerve crush 2 weeks later. Zymosan (Sigma Aldrich; 12.5 μg/μL) along with the cAMP analog CPT-cAMP (Sigma; 50 μM, 3 μL) was injected as described (de Lima et al, 2012). Zymosan and CPT-cAMP were injected intravitreally immediately after crush injury, and additional Zymosan at half the original dose plus CPT-cAMP at the original dose again 3 and 6 wk later. For each intravitreal injection, a glass micropipette was inserted into the peripheral retina, just behind the ora serrata, and was deliberately angled to avoid damage to the lens. For optic nerve crush injury, the optic nerve was exposed intraorbitally and crushed with jeweler's forceps (Dumont #5; tip dimension, 0.1 × 0.06 mm) for 5 seconds approximately 1 mm behind the optic disc. Using retrograde and anterograde experiments, completeness of axotomy has been confirmed in our previous study (Park et al, 2008). Two to 7 days before sacrifice, l–2 μl of cholera toxin β subunit (CTB)-Alexa 555 (2 μg/μl, Invitrogen) was injected into the vitreous with a Hamilton syringe (Hamilton) to anterogradely label regenerating RGC axons. *ALDH1L1-EGFP* (Doyle et al, 2008; Yang et al, 2011) *, PLP-EGFP* (Mallon et al, 2002) and *CX3CR1-EGFP* mice (Jung et al, 2000) received unilateral optic nerve crush. At 14–17 days later, optic nerves from these transgenic mice were treated for tissue clearance and analyzed for the distribution of glial cells in the injured optic nerve. Uninjured mice (C57BL/6 at 5 weeks old) with bilateral CTB tracing received intravitreal CTB-555 injection in the right eye and CTB-488 injection in the left eye.

AAVs

cDNA of Cre was inserted downstream of the CMV promoter/β-globin intron enhancer in the plasmid pAAV-MCS (Stratagene), containing the AAV2 inverted terminal repeats and a human growth hormone polyA signal. pAAV-RC (Stratagene) that encodes the AAV2 genes (rep and cap) and the helper plasmid (Stratagene) that encodes E2A, E4 and VA were used for cotransfection of 293T cells to generate recombinant AAV. AAV2 viral particles were prepared by the University of Miami Viral Vector Core using an FPLC method to produce titers of approximately 4×10^{13} particles/ml.

Tissue preparation and clearing

Mice were perfused transcardially with PBS followed by 4% paraformaldehyde (PFA) in phosphate buffered saline (PBS) at 5 ml/min. The optic nerve and the brain were dissected and post-fixed with 4% PFA in PBS overnight. For histological sectioning, samples were cryoprotected by incubating in 30% sucrose overnight. For tissue clearing, samples were rinsed with PBS and stored at 4°C until needed. Tissue clearing was performed as described (Becker et al, 2012; Erturk et al, 2012), with minor modifications. Samples underwent dehydration by incubation in increasing concentration of THF (Sigma-Aldrich) solutions under constant rocking. Optic nerves were incubated in 50% THF (diluted in water v/v), 80% THF (v/v) and 100% THF for 15 minutes each. Dehydrated optic nerve was rendered clear by incubating in BABB (a mixture of benzyl alcohol and benzyl benzoate (Sigma-Aldrich) at a ratio of 1:2) for 20 minutes. Adult mouse brain was incubated in 50% THF for 12 hours, 80% THF for 12 hours, 100% THF for 3 × 12 hours, and BABB for 12 hours before imaging.

LSFM (ultramicroscopy)

Ultramicroscope illuminates specimen with a thin sheet of light formed by two lenses, allowing imaging of large tissues, yet with cellular resolution (Fig. 1C). Ultramicroscopy was performed as previously described (Erturk et al, 2012). Between 100 to 500 optical slices were imaged. The scan speed was 0.5–1.5 s per section, which was about 2–3 minutes for the optic nerve and 5–10 minutes for the brain for a complete scan of the tissue. Images were collected at 2 to 5μm increment in Z axis.

Image processing, neurite tracing and statistical analysis

Images, videos and 3D volume rendering were prepared using Imaris software v7.6.1 (Bitplane). CTB-labeled RGC axons in the optic nerve and brain were traced using Imaris Filament Tracer Module. To quantify the number of axons that regenerated long distances in the optic nerve, we counted the CTB-labeled fibers that crossed different distances from the lesion site after scanning through 100 to 200 individual horizontal optical slices. To quantify the number of axons that extended into different regions beyond the optic chiasm, we counted the CTB-labeled fibers that were found in the optic tracts, opposite optic nerve and hypothalamus after scanning through 100 to 300 individual horizontal optical slices. We used Student's t test for two group comparisons using SPSS statistics software.

RESULTS

3D visualization of RGC axonal projections in uninjured mouse

In this study, we set out to apply tissue clearance and LSFM to evaluate regeneration of RGC axons without histological sectioning. Initially we visualized RGC axonal projections in the whole brain of uninjured animal. Adult mice received intravitreal injection of fluorophore-conjugated CTB, a lipophilic tracer used routinely to label CNS axons in regeneration studies. Seven days later, samples were processed for tissue clearance. THF-based clearing methods rendered mouse optic nerve and brain transparent to a large extent (Fig. 1A and B). A total of 1 hour incubation in THF/BABB solutions was sufficient to clear the optic nerve, while it took approximately 3 days for the brain. Normally, RGCs send axons to central targets including the lateral geniculate nucleus (LGN) and superior colliculus (SC), which are involved in image-forming visual functions. RGC axons also innervate the suprachiasmatic nucleus (SCN) and olivary pretectal nucleus (OPT) that are involved in non-image forming visual functions. After imaging the entire depth of the brain, approximately 500 optical slices (Movie 1) were compiled using Imaris software for 3D reconstruction. RGC axons can be visualized in 3D with remarkable detail along the entire visual pathway through the optic nerve, chiasm and optic tracts to the SCN, OPT, LGN, and SC (Fig. 1D–I, Movies 1 and 2). In mice, a small proportion of RGCs located in the ventro-temporal retina send their axons to the ipsilateral brain. The ipsilateral projection stemming from the optic chiasm to the various brain regions is clearly visible (Movie 2), with axons terminating in the dorsal and ventral LGN (Fig. 1D–I), and in the different layers of the SC (Fig. 1H). We also detected several RGC axons (10–30 axons; n=4) that turn at the optic chiasm and project to the opposite optic nerve (Fig. 1G), confirming that some axons are misrouted at the chiasm during development (Bunt et al, 1983). Together, we show that tissue clearance combined with LSFM allows 3D visualization of the entire optic pathway as well as single axons that leave the main bundle, providing excellent details regarding the paths taken by RGC axons.

3D assessment of regenerating axons shows high degree of axon turning

Next, we assessed regenerating RGC axons following injury. To this end, we analyzed animals with genetic deletion of PTEN/SOCS3 in adult RGCs, together with intravitreal

injection of CNTF, a condition known to promote long distance regeneration of many RGC axons after an optic nerve crush (Sun et al, 2011). Adult PTEN/SOCS3$^{f/f}$ mice received intravitreal injection of AAV2-Cre to induce PTEN/SOCS3 deletion in adult RGCs, followed by an intraorbitral crush injury 2 weeks later (Sun et al, 2011). Animals received CNTF injection on the day of injury, at 3 days post-injury, and bi-weekly thereafter. Previously, we have demonstrated that AAV2-Cre at appropriate viral titers infects the majority of RGCs in adult mice (Park et al, 2008; Sun et al, 2011). Control animals received AAV-GFP injection. Two days prior to sacrifice, animals received CTB injection to label regenerating RGC axons. In control animals, a few axons sprouted short distances at the lesion site, but no axons were found beyond 1 mm from the lesion site at 17 days post-injury (n=5; Fig. 2A, Movie 3). On the other hand, many axons extended into and beyond the lesion in PTEN/SOCS3 KO mice (Fig. 2A and E, Movie 4). The use of LSFM allowed comprehensive evaluation of three different aspects of axon growth that are difficult to obtain in histological sections. First, LSFM allowed direct counting of almost all fibers that have regenerated long distances through the optic nerve. By scanning through individual optical slices (i.e. z-stack images taken at 2–5 μm increments; a total of 150–200 optical slices/optic nerve), we could count individual CTB labeled fibers crossing different distances distal to the lesion site in PTEN/SOCS3 KO mice (n=5; Fig. 2E). Second, it allowed unequivocal examination of the axonal trajectories along their regenerative paths, and where the regenerated axons terminate. Notably, we found that while a few RGC axons project relatively straight towards the brain (Fig. 2B), most axons have a meandering path. Many axons made sharp turns (often multiple occasions) with some axons reversing course and projecting towards the eye (Fig. 2C & Movie 4). These results are consistent with a recent study by Pernet et al., in which many axons induce to regenerate following elevation of CNTF were shown to take circuitous paths in the optic nerve (Pernet et al, 2012). We noticed in our study that these “turning events” seemed highly prevalent in the proximal nerve regions close to the lesion site. We traced the paths of axons (a total of 80 axons) within this proximal nerve region (i.e. a region covering 0.2 – 0.4 mm distal to the optic nerve head) and found that about 40 % of axons made at least one U-turn (Fig. 2F). On the other hand, only about 10% of regenerating axons made U-turn in the more distal nerve region (i.e. 1 – 1.2 mm distal to the optic nerve head; Fig. 2F). We performed optic nerve crush in transgenic mice in which astrocytes, oligodendrocytes or microglial cells are labeled with EGFP to examine the correlation between the presence of glial cells and axon turning (Supplementary Fig. 1). After LSFM, we observed high astrocyte density in the proximal region of the optic nerve close to the lesion site in ALDH1L1-EGFP mice (n=3; Supplementary Fig. 1). These results suggest that the nerve region with a high degree of axon turning may correspond to the areas with strong astroglial activation. Third, 3D visualization provided detailed examination of the axonal morphologies. For instance, it is clear that some RGC axons generate branches as they re-grow along the optic nerve (Fig. 2*D* & Movie 4), a morphogenetic process normally found in growing axons during nervous system development. Approximately 10–20% of axons traced in PTEN/SOCS3 KO showed at least one axonal branch. Together, we demonstrate that at present, tissue clearance combined with LSFM represents the most precise method to assess RGC axon regeneration, allowing unequivocal assessment of axonal trajectories and growth patterns in the optic nerve.

3D assessment of axonal projections to the brain

Recent studies from us and others demonstrated that PTEN KO alone or in combination with other strategies, such as SOCS3 deletion, promote long distance axon regeneration, with RGC axons projecting to the brain (de Lima et al, 2012; Kurimoto et al, 2010; Sun et al, 2011). Because histological sections provide incomplete spatial information about axonal trajectory and where RGC axons terminate in the brain, we applied LSFM to examine

axonal projections in the brain. After imaging the entire brain, approximately 500 optical slices were compiled using Imaris software for 3D reconstruction. At 10 weeks post-injury, RGC axons were not detected in the optic chiasm or brain of AAV-GFP control animals (data not shown). In PTEN/SOCS3 KO animals however, many CTB-labeled regenerating axons reached the optic nerve/chiasm transition zone (OCTZ) (a mean of 119 fibers/animal; n=8; SEM=16.5). To evaluate the axonal projections through the optic chiasm and to the brain, we measured the number of axons projecting to different brain regions. In all animals examined (n=8), similar or higher numbers of axons were found in the ipsilateral optic tract than in the contralateral optic tract (Fig. 3E and *G*, Movie 5). In all animals, we observed that a small percentage of RGC axons also extend into the opposite uninjured optic nerve (Fig. 3E and G, Movie 5). Some axons appeared to be inhibited from entering the OCTZ, or turn sharply at the OCTZ before continuing to project into the optic tracts (Fig. 3B). In the brain, a few axons extended medial-dorsally into the hypothalamic brain regions including the SCN and medial pre-optic area, while some axons exited the optic tracts to reach the lateral hypothalamus (Fig. 3C and D, Supplementary Fig. 2). In some animals, we found regenerating axons in abnormal regions that are not typically associated with the optic pathway including the fornix and extended amygdala (unpublished data). RGC axons were not detected in the more distant visual targets including LGN or SC (Fig. 3, Supplementary Fig. 2, Movie 5). We also examined axon regeneration in animals subjected to shorter and longer survival times (i.e. 8 and 16 weeks after injury; unpublished data). However, among these time points, we observed the greatest degree of axon regeneration (i.e. axon number and length in the brain) in the brain at 10 weeks post-injury time point.

To ensure that the axonal projections observed using LSFM are not under-represented by potential loss of CTB signal during the clearing procedure, LSFM results were corroborated by examining fibers in coronal brain sections from a separate set of animals (n=8). In coronal sections, CTB-labeled RGC axons were found mainly in the hypothalamus region including the SCN, anterior hypothalamic area and ventromedial hypothalamus (Supplementary Fig. 2). Laterally, some axons travelled short distances within the degenerated optic tracts. RGC axons were not found in the more distant targets, LGN and SC (Supplementary Fig. 2). Immunohistochemical staining of the brain sections using CTB antibody to amplify the signal did not detect regenerated axons in midbrain targets, LGN and SC.

3D assessment of axonal projection in PTEN KO/ Zymosan/cAMP analogue-treated mice

It was recently reported that PTEN KO combined with Zymosan and the cAMP analogue (PTEN KO/ZYM/cAMP) promotes extensive long distance regeneration of RGC axons. Strikingly, regenerating RGC axons in these mice were reported to re-innervate all the major visual targets including the OPT, LGN and SC (de Lima et al, 2012). Thus, we applied LSFM to examine axon regeneration to the brain in PTEN KO/ZYM/cAMP mice. Adult $PTEN^{f/f}$ mice received an intravitreal AAV-Cre injection 2 weeks prior to a crush injury, and Zymosan and the cAMP analogue were administered during the survival time as previously described (de Lima et al, 2012). At 10 to 12 weeks after injury, the optic nerves and brains were cleared using THF and imaged with the LSFM. Five to 7 days prior to sacrifice, CTB was injected to label the regenerating axons. As expected, many axons regenerated long distances in the optic nerve of the PTEN KO/ZYM/cAMP mice (Fig. 4B). Similar to the axon number reported previously (de Lima et al, 2012), many RGC axons (a mean of 112 fibers/animal; n=9; SEM=19.5) elongated long distances (4–5 mm distal to the lesion site) to reach the optic chiasm (Fig. 4B). In the brain, the axonal projection was similar to that of PTEN/SOCS3 KO mice. In general, similar or higher numbers of axons were found in the ipsilateral optic tract than in the contralateral optic tract (Fig. 4E and G). A few RGC axons extended into the opposite uninjured optic nerve (Fig. 4E and G), while

others projected dorsally to the SCN (Supplementary Fig 3). Some axons also exited the optic tracts and extended into the lateroanterior hypothalamic nucleus or supraoptic nucleus. RGC axons were not detected in the OPT, LGN and SC (Supplementary Fig. 3).

3D assessment of axonal projections following bilateral optic nerve crush

The optic chiasm is a region where RGC axons from each eye meet (Movie 6). As previously mentioned, some regenerating axons made sharp turns upon reaching the optic chiasm, suggesting that intact axons from the contralateral eye may affect the trajectory of regenerating axons in this region. To examine this possibility, we carried out a bilateral crush experiment. AAV-Cre/rCNTF was injected into the left eye of PTEN/SOCS3 floxed mice, followed by crush on both optic nerves 2 weeks later. At 10 weeks after bilateral crush injury, we observed that while similar numbers of axons regenerated up to the optic chiasm compared to the animals receiving a unilateral crush, higher numbers of axons regenerated into and beyond the optic chiasm. However, the overall trajectory pattern at the optic chiasm was similar compared to unilateral crush. Similar or higher numbers of axons extended into the ipsilateral optic tract than to the contralateral optic tract, with a few axons extending also into the opposite optic nerve. Some axons projected dorsally to reach the SCN, or medial pre-optic area (Fig. 5).

DISCUSSION

We have applied tissue clearance and LSFM to obtain a comprehensive assessment of RGC axon regeneration after injury. Using these methods, we were able to image the entire mouse optic nerve and brain, providing 3D visualization of the optic pathways from the eye through the brain. This approach allowed not only visualization of the main axon bundles that make up the visual pathway in normal animals, but it also enabled detection of single axons that leave the main pathway to stream into aberrant regions. For instance, in all uninjured control mice examined, between 10–30 axons were found to turn at the optic chiasm and project long distances into the contralateral optic nerve, confirming that some RGC axons are misrouted at the chiasm during development and persist in the adult (Bunt et al, 1983). Thus, these results highlight the strength of 3D imaging to detect small numbers of axons that would have been difficult to identify in histological sections. In addition to observing axonal trajectories, we also found that some RGC axons generate branches as they regenerate. During development, RGC axons generate branches to connect with multiple synaptic targets, a process known to be regulated in part by target-derived trophic factors such as nerve growth factor and brain derived neurotrophic factor (Gibson & Ma, 2011). Although some regenerated axons in our study generated branches prematurely within optic nerve, other axons generated branches in the hypothalamus, raising the possibility that the regenerated axons could, in principle, re-establish connections with multiple synaptic targets in the adults. LSFM also allowed more accurate determination of regenerating fiber numbers. While it was challenging to directly count the axons close to the lesion because of the dense axonal projection, we were able to directly count virtually all axons that regenerated long distances.

To innervate the visual targets in the brain, regenerating RGC axons must travel long distance along the optic nerve and then correctly pathfind through various regions in the brain. While it has been a major challenge to develop strategies that stimulate RGC axons to regenerate long distances in the first place, studies over the past several years have shown that this is feasible, at least for some RGCs. For example, in adult Bcl-2tg mice, virally-induced over-expression of CNTF promotes long distance regeneration to the optic chiasm (Leaver et al, 2006). Very recently, Pernet et al., demonstrated that the expression of CNTF using AAV2 alone induces long distance regeneration of RGC axons in wild type mice (Pernet et al, 2012). In addition, PTEN deletion in RGCs, combined with SOCS3 deletion/

CNTF injection (Sun et al, 2011), or with Zymosan and cAMP analogue (de Lima et al, 2012; Kurimoto et al, 2010) promoted extensive long distance regeneration in the optic nerve, allowing some RGC axons to reach into the brain. Using LSFM, we observed that many axons grew in tortuous paths in the optic nerve, making multiple turns, and often projecting back to the eye. Thus, our data are in agreement with the recent study from Pernet et al., in which extensive axon turning was evident in optic nerves of animals treated with AAV-CNTF (Pernet et al, 2012). Collectively, these studies indicate that there is considerable axon misguidance within the injured optic nerve during regeneration, which may limit some RGC axons extending into the brain and ultimately to their targets.

During development, *de novo* RGC axons enter the optic nerve and travel in a fasciculated manner towards the brain. This process is tightly regulated by signaling molecules expressed and released by neuronal and non-neuronal cells in the interstitial spaces and the extracellular matrix. For example, Sema5A which is found on neuroepithelial cells surrounding the retinal axons along the optic nerve, was shown to induce growth cone collapse, and antibodies against SemaA5 causes retinal axons to escape from the optic nerve bundle (Oster et al, 2003). Other axon repulsive cues such as myelin associated glycoproteins, semaphorins, ephrins, chondroitin sulfate proteoglycans (CSPGs) and their respective receptors have also been shown to be expressed in the injured retina and optic nerve (Cai et al, 2012; Du et al, 2007; Goldberg et al, 2004; Hunt et al, 2003; Liu et al, 2006; Park et al, 2008; Selles-Navarro et al, 2001; Shirvan et al, 2002), and could, in principle, contribute to the heterogeneous axon growth patterns seen in the optic nerves. In ALDH1L1-EGFP tg mice in which astrocytes are labeled with EGFP, strong astroglial activation is seen in the nerve regions close to the lesion site. Given that axon turning in PTEN/SOCS3 KO mice was especially prevalent in these regions, it is plausible that high concentration of CSPGs and other repulsive factors (or growth factors) released by reactive astrocytes may contribute to the extensive axon turning. It is currently unclear to what extent these and other growth inhibitory (or attractive) cues present in the injured optic nerve contribute to the aberrant axon trajectories observed in the adult optic nerve.

One major decision point for growing RGC axons en route to their central targets is the optic chiasm where axons must decide whether or not to cross. The majority of animals in our study had similar or higher numbers of axons extending to the ipsilateral side of the brain than the contralateral side. This observation is consistent with the previous report demonstrating large ipsilateral projections of regenerating RGC axons in perinatal Bcl-2 transgenic mice (Cho et al, 2005). Potentially, intact RGC axons from the opposite eye could affect the course of growing axons at the optic chiasm. For instance, previous studies in frogs have demonstrated that the number of axons that regenerate to the opposite nerve is less in animals subjected to a bilateral optic nerve lesion compared to unilaterally lesioned animals (Bohn & Stelzner, 1981). On the other hand, studies using a prechiasmic lesion in adult rats showed no obvious difference in the divergence patterns of regenerating axons at the optic chiasm between animals subjected to bilateral and unilateral crush (Berry et al, 1999). Consistent with this latter study, the overall divergence pattern at the optic chiasm was similar in both of our injury models in mice, supporting the idea that interactions between regenerating axons and the intact axons from the uninjured eye may not be responsible for establishing the aberrant trajectories.

Axonal pathfinding at the optic chiasm during development is regulated by EphB1/ephrinB2 signaling: the Ephb1 receptor is expressed in a small population of RGCs, and axons extending from these RGCs are repelled by ephrinB2 ligand expressed in the chiasm midline, thus giving rise to the ipsilateral projection (Williams et al, 2003). Other guidance cues and receptors involved in pathfinding through the chiasm during nervous system development include Zic2, NrCAM, Islet-1, Plexin-A1 and semaphorin6D (Herrera et al,

2003; Kuwajima et al, 2012; Pak et al, 2004; Petros et al, 2008; Williams et al, 2006). The expression levels of Eph1B and ephrinB2 in the adult mouse retina and optic chiasm, and whether the higher percentage of ipsilaterally projecting axons seen in these studies are due to EphB1/ephrinB2 signaling or other aforementioned guidance factors is not yet known. Nonetheless, our results indicate that the molecular and cellular mechanisms that once guided axons through the optic chiasm during development are not preserved in adult mice.

With the recent progress made in promoting long distance regeneration in the optic nerve, a pressing question is to what extent do these axons navigate correctly to re-innervate their central targets? In both PTEN/SOCS3 KO and PTEN KO/ZYM/cAMP mice, RGC axons projected dorsally into the hypothalamus or short distances laterally to the optic tracts or projected to the uninjured contralateral optic nerve. Centrally, axonal projections were limited primarily to the hypothalamus. Thus, our findings are in contrast to the previous study using PTEN KO/ZYM/cAMP mice in which many regenerating axons were reported to elongate long distances within the brain, correctly navigating and re-innervating all the major visual targets including the SCN, OPT, MTN, LGN and SC (de Lima et al, 2012). The reasons behind these differing results are not clear. Of note, in this present study, similar number of axons regenerated long distances up to the optic chiasm in the PTEN KO/Zym/cAMP treated mice as reported previously (de Lima et al, 2012), confirming the effectiveness of this combinatorial approach in promoting RGC axon regeneration.

In nearly all animals, regenerating axons were found in the SCN, the master pacemaker of circadian rhythm. In normal mammals, the SCN receives axons predominantly from melanopsin expressing-intrinsically photosensitive RGCs (ipRGCs). These RGCs directly send photic information to the SCN which in turn regulates daily rhythmicity such as sleep, body temperature and food intake (Do & Yau, 2010; Schmidt et al, 2011). This raises questions as to whether or to what extent the regenerated RGC axons found in the SCN originate from the ipRGCs, and whether they form functional synaptic connections with the SCN neurons. In addition, our results demonstrated some axons generated branches, raising a question as to whether axonal branching during regeneration is a feature unique to a specific RGC subset, or occurs at random in any regenerating RGC axon. The combined use of tissue clearance and 3D visualization together with transgenic mice in which axons from known subtypes of RGCs are GFP-labeled may facilitate addressing these questions. In summary, we demonstrated, for the first time, integration of tissue clearance and LSFM for comprehensive analysis of RGC axon regeneration in mouse models. Our study shows misdirected growth in the optic nerve and brain, indicating that the adult mammalian CNS lacks the signals necessary for proper pathfinding of regenerating RGC axons.

Supplementary Material

Refer to Web version on PubMed Central for supplementary material.

Acknowledgments

This work was supported by grants from U.S Army W81XWH-05-1-0061 (VPL, PT, KKP), NIH HD057521 (VPL), U.S Army W81XWH-12-1-0319 (KKP), NEI 1R01EY022961-01 (KKP), Ziegler Foundation (KKP), Pew Charitable Trust (KKP) and the Miami Project to Cure Paralysis and Buoniconti Fund (VPL, PT, KKP). VPL holds the Walter G Ross Distinguished Chair in Developmental Neuroscience. We thank the Imaging Core at the Miami Project to Cure Paralysis for the LSFM facility, and Drs. Daniel Liebl, Jae Lee, Jeffrey Rothstein and Wendy Macklin for providing the transgenic mice.

References

Beazley LD, Sheard PW, Tennant M, Starac D, Dunlop SA. Optic nerve regenerates but does not restore topographic projections in the lizard Ctenophorus ornatus. J Comp Neurol. 1997; 377:105–120. [PubMed: 8986876]

Becker CG, Becker T. Growth and pathfinding of regenerating axons in the optic projection of adult fish. J Neurosci Res. 2007; 85:2793–2799. [PubMed: 17131420]

Becker K, Jahrling N, Saghafi S, Weiler R, Dodt HU. Chemical clearing and dehydration of GFP expressing mouse brains. PLoS One. 2012; 7:e33916. [PubMed: 22479475]

Berry M, Carlile J, Hunter A, Tsang W, Rosenstiel P, Sievers J. Optic nerve regeneration after intravitreal peripheral nerve implants: trajectories of axons regrowing through the optic chiasm into the optic tracts. J Neurocytol. 1999; 28:721–741. [PubMed: 10859575]

Bohn RC, Stelzner DJ. The aberrant retino-retinal projection during optic nerve regeneration in the frog. III. Effects of crushing both nerves. J Comp Neurol. 1981; 196:633–643. [PubMed: 6970758]

Bunt SM, Lund RD, Land PW. Prenatal development of the optic projection in albino and hooded rats. Brain Res. 1983; 282:149–168. [PubMed: 6831237]

Cai X, Yuan R, Hu Z, Chen C, Yu J, Zheng Z, Ye J. Expression of PirB protein in intact and injured optic nerve and retina of mice. Neurochem Res. 2012; 37:647–654. [PubMed: 22102155]

Cho KS, Yang L, Lu B, Feng Ma H, Huang X, Pekny M, Chen DF. Reestablishing the regenerative potential of central nervous system axons in postnatal mice. J Cell Sci. 2005; 118:863–872. [PubMed: 15731004]

de Lima S, Koriyama Y, Kurimoto T, Oliveira JT, Yin Y, Li Y, Gilbert HY, Fagiolini M, Martinez AM, Benowitz L. Full-length axon regeneration in the adult mouse optic nerve and partial recovery of simple visual behaviors. Proc Natl Acad Sci U S A. 2012; 109:9149–9154. [PubMed: 22615390]

Do MT, Yau KW. Intrinsically photosensitive retinal ganglion cells. Physiol Rev. 2010; 90:1547–1581. [PubMed: 20959623]

Doyle JP, Dougherty JD, Heiman M, Schmidt EF, Stevens TR, Ma G, Bupp S, Shrestha P, Shah RD, Doughty ML, Gong S, Greengard P, Heintz N. Application of a translational profiling approach for the comparative analysis of CNS cell types. Cell. 2008; 135:749–762. [PubMed: 19013282]

Du J, Tran T, Fu C, Sretavan DW. Upregulation of EphB2 and ephrin-B2 at the optic nerve head of DBA/2J glaucomatous mice coincides with axon loss. Invest Ophthalmol Vis Sci. 2007; 48:5567–5581. [PubMed: 18055806]

Duffy P, Wang X, Seigel CS, Tu N, Henkemeyer M, Cafferty WB, Strittmatter SM. Myelin-derived ephrinB3 restricts axonal regeneration and recovery after adult CNS injury. Proc Natl Acad Sci U S A. 2012

Erturk A, Mauch CP, Hellal F, Forstner F, Keck T, Becker K, Jahrling N, Steffens H, Richter M, Hubener M, Kramer E, Kirchhoff F, Dodt HU, Bradke F. Three-dimensional imaging of the unsectioned adult spinal cord to assess axon regeneration and glial responses after injury. Nat Med. 2012; 18:166–171. [PubMed: 22198277]

Gibson DA, Ma L. Developmental regulation of axon branching in the vertebrate nervous system. Development. 2011; 138:183–195. [PubMed: 21177340]

Goldberg JL, Vargas ME, Wang JT, Mandemakers W, Oster SF, Sretavan DW, Barres BA. An oligodendrocyte lineage-specific semaphorin, Sema5A, inhibits axon growth by retinal ganglion cells. J Neurosci. 2004; 24:4989–4999. [PubMed: 15163691]

Groszer M, Erickson R, Scripture-Adams DD, Lesche R, Trumpp A, Zack JA, Kornblum HI, Liu X, Wu H. Negative regulation of neural stem/progenitor cell proliferation by the Pten tumor suppressor gene in vivo. Science. 2001; 294:2186–2189. [PubMed: 11691952]

Herrera E, Brown L, Aruga J, Rachel RA, Dolen G, Mikoshiba K, Brown S, Mason CA. Zic2 patterns binocular vision by specifying the uncrossed retinal projection. Cell. 2003; 114:545–557. [PubMed: 13678579]

Hunt D, Coffin RS, Prinjha RK, Campbell G, Anderson PN. Nogo-A expression in the intact and injured nervous system. Mol Cell Neurosci. 2003; 24:1083–1102. [PubMed: 14697671]

Jung S, Aliberti J, Graemmel P, Sunshine MJ, Kreutzberg GW, Sher A, Littman DR. Analysis of fractalkine receptor CX(3)CR1 function by targeted deletion and green fluorescent protein reporter gene insertion. Mol Cell Biol. 2000; 20:4106–4114. [PubMed: 10805752]

Kurimoto T, Yin Y, Omura K, Gilbert HY, Kim D, Cen LP, Moko L, Kugler S, Benowitz LI. Long-distance axon regeneration in the mature optic nerve: contributions of oncomodulin, cAMP, and pten gene deletion. J Neurosci. 2010; 30:15654–15663. [PubMed: 21084621]

Kuwajima T, Yoshida Y, Takegahara N, Petros TJ, Kumanogoh A, Jessell TM, Sakurai T, Mason C. Optic chiasm presentation of Semaphorin6D in the context of Plexin-A1 and Nr-CAM promotes retinal axon midline crossing. Neuron. 2012; 74:676–690. [PubMed: 22632726]

Leaver SG, Cui Q, Plant GW, Arulpragasam A, Hisheh S, Verhaagen J, Harvey AR. AAV-mediated expression of CNTF promotes long-term survival and regeneration of adult rat retinal ganglion cells. Gene Ther. 2006; 13:1328–1341. [PubMed: 16708079]

Lingor P, Tonges L, Pieper N, Bermel C, Barski E, Planchamp V, Bahr M. ROCK inhibition and CNTF interact on intrinsic signalling pathways and differentially regulate survival and regeneration in retinal ganglion cells. Brain. 2008; 131:250–263. [PubMed: 18063589]

Liu X, Hawkes E, Ishimaru T, Tran T, Sretavan DW. EphB3: an endogenous mediator of adult axonal plasticity and regrowth after CNS injury. J Neurosci. 2006; 26:3087–3101. [PubMed: 16554460]

Mallon BS, Shick HE, Kidd GJ, Macklin WB. Proteolipid promoter activity distinguishes two populations of NG2-positive cells throughout neonatal cortical development. J Neurosci. 2002; 22:876–885. [PubMed: 11826117]

Moore DL, Blackmore MG, Hu Y, Kaestner KH, Bixby JL, Lemmon VP, Goldberg JL. KLF family members regulate intrinsic axon regeneration ability. Science. 2009; 326:298–301. [PubMed: 19815778]

Muller A, Hauk TG, Fischer D. Astrocyte-derived CNTF switches mature RGCs to a regenerative state following inflammatory stimulation. Brain. 2007; 130:3308–3320. [PubMed: 17971355]

Oster SF, Bodeker MO, He F, Sretavan DW. Invariant Sema5A inhibition serves an ensheathing function during optic nerve development. Development. 2003; 130:775–784. [PubMed: 12506007]

Pak W, Hindges R, Lim YS, Pfaff SL, O'Leary DD. Magnitude of binocular vision controlled by islet-2 repression of a genetic program that specifies laterality of retinal axon pathfinding. Cell. 2004; 119:567–578. [PubMed: 15537545]

Park KK, Liu K, Hu Y, Smith PD, Wang C, Cai B, Xu B, Connolly L, Kramvis I, Sahin M, He Z. Promoting axon regeneration in the adult CNS by modulation of the PTEN/mTOR pathway. Science. 2008; 322:963–966. [PubMed: 18988856]

Paxinos, G.; Franklin, KBJ. The mouse brain in stereotaxic coordinates. Compact 2nd edn.. Amsterdam: Boston: Elsevier Academic Press; 2004.

Pernet V, Joly S, Dalkara D, Jordi N, Schwarz O, Christ F, Schaffer DV, Flannery JG, Schwab ME. Long-distance axonal regeneration induced by CNTF gene transfer is impaired by axonal misguidance in the injured adult optic nerve. Neurobiol Dis. 2012

Petros TJ, Rebsam A, Mason CA. Retinal axon growth at the optic chiasm: to cross or not to cross. Annu Rev Neurosci. 2008; 31:295–315. [PubMed: 18558857]

Qiu J, Cai D, Filbin MT. A role for cAMP in regeneration during development and after injury. Prog Brain Res. 2002; 137:381–387. [PubMed: 12440380]

Schmidt TM, Chen SK, Hattar S. Intrinsically photosensitive retinal ganglion cells: many subtypes, diverse functions. Trends Neurosci. 2011; 34:572–580. [PubMed: 21816493]

Selles-Navarro I, Ellezam B, Fajardo R, Latour M, McKerracher L. Retinal ganglion cell and nonneuronal cell responses to a microcrush lesion of adult rat optic nerve. Exp Neurol. 2001; 167:282–289. [PubMed: 11161616]

Shirvan A, Kimron M, Holdengreber V, Ziv I, Ben-Shaul Y, Melamed S, Melamed E, Barzilai A, Solomon AS. Anti-semaphorin 3A antibodies rescue retinal ganglion cells from cell death following optic nerve axotomy. J Biol Chem. 2002; 277:49799–49807. [PubMed: 12376549]

Smith PD, Sun F, Park KK, Cai B, Wang C, Kuwako K, Martinez-Carrasco I, Connolly L, He Z. SOCS3 deletion promotes optic nerve regeneration in vivo. Neuron. 2009; 64:617–623. [PubMed: 20005819]

Stelzner DJ, Bohn RC, Strauss JA. Regeneration of the frog optic nerve. Comparisons with development. Neurochem Pathol. 1986; 5:255–288. [PubMed: 3306474]

Su Y, Wang F, Zhao SG, Pan SH, Liu P, Teng Y, Cui H. Axonal regeneration after optic nerve crush in Nogo-A/B/C knockout mice. Mol Vis. 2008; 14:268–273. [PubMed: 18334965]

Sun F, Park KK, Belin S, Wang D, Lu T, Chen G, Zhang K, Yeung C, Feng G, Yankner BA, He Z. Sustained axon regeneration induced by co-deletion of PTEN and SOCS3. Nature. 2011; 480:372–375. [PubMed: 22056987]

Williams SE, Grumet M, Colman DR, Henkemeyer M, Mason CA, Sakurai T. A role for Nr-CAM in the patterning of binocular visual pathways. Neuron. 2006; 50:535–547. [PubMed: 16701205]

Williams SE, Mann F, Erskine L, Sakurai T, Wei S, Rossi DJ, Gale NW, Holt CE, Mason CA, Henkemeyer M. Ephrin-B2 and EphB1 mediate retinal axon divergence at the optic chiasm. Neuron. 2003; 39:919–935. [PubMed: 12971893]

Winzeler AM, Mandemakers WJ, Sun MZ, Stafford M, Phillips CT, Barres BA. The lipid sulfatide is a novel myelin-associated inhibitor of CNS axon outgrowth. J Neurosci. 2011; 31:6481–6492. [PubMed: 21525289]

Wong EV, David S, Jacob MH, Jay DG. Inactivation of myelin-associated glycoprotein enhances optic nerve regeneration. J Neurosci. 2003; 23:3112–3117. [PubMed: 12716917]

Yang Y, Vidensky S, Jin L, Jie C, Lorenzini I, Frankl M, Rothstein JD. Molecular comparison of GLT1+ and ALDH1L1+ astrocytes in vivo in astroglial reporter mice. Glia. 2011; 59:200–207. [PubMed: 21046559]

Highlights

- Use of light sheet fluorescence microscope for analysis of retinal axon re-growth.
- Provided in-depth 3D assessment of axonal trajectories in the optic nerve and brain.
- Demonstrated significant misdirection of retinal axons following regeneration.
- Highlighted lack of axonal path-finding in adult visual system after injury.

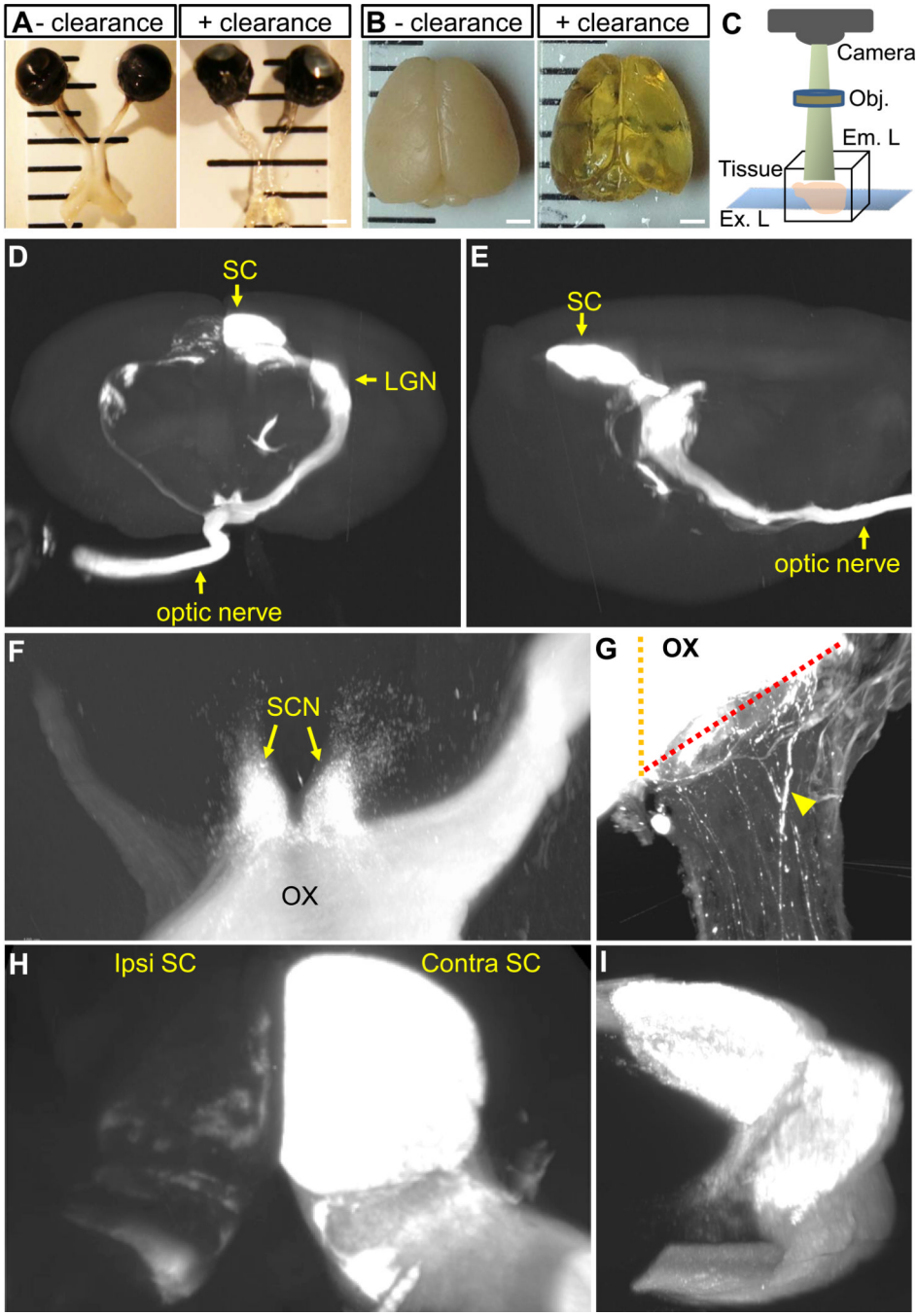

Figure 1.

Tetrahydrofuran (THF)-based tissue clearing and LSFM methods allow 3D visualization of RGC axonal projections in whole tissue. **A**, adult mouse optic nerve and chiasm, and **B**, whole brain before and after clearance with THF and BABB. **C**, Principle of LSFM. Optic nerves and brains were cleared, and then imaged under an Ultramicroscope (LaVision Biotec). Horizontal optical slices were compiled using Imaris software for 3D reconstruction. **D–I**, snapshot images from 3D reconstruction video. Anterior, **D** and lateral, **E** views of a cleared brain displaying the trajectory of CTB-labeled RGC axons from the eye, through the chiasm and into the brain. All visual targets including the suprachiasmatic

nucleus, lateral geniculate nucleus and superior colliculus both in the ipsilateral and contralateral sides of the brain can be clearly visualized. **F–I**, higher magnification images taken from 3D reconstruction showing axonal projections to the chiasm and SCN, and diverging into the ipsilateral and contralateral optic tracts in **F**, to the opposite optic nerve in **G** (arrowhead indicates CTB-labeled axons), ipsilateral and contralateral superior colliculus in **H**, and contralateral lateral geniculate nucleus in **I**. In **G**, yellow and red dotted lines represent the chiasm midline and the optic nerve-chiasm transition zone, respectively. Ex. L, excitation light; Em. L, emission light; Obj, objective; SC, superior colliculus; SCN, suprachiasmatic nucleus; LGN, lateral geniculate nucleus; ipsi, ipsilateral; contra, contralateral; OX, optic chiasm. Scale bars, 1 mm in **A** and **B**.

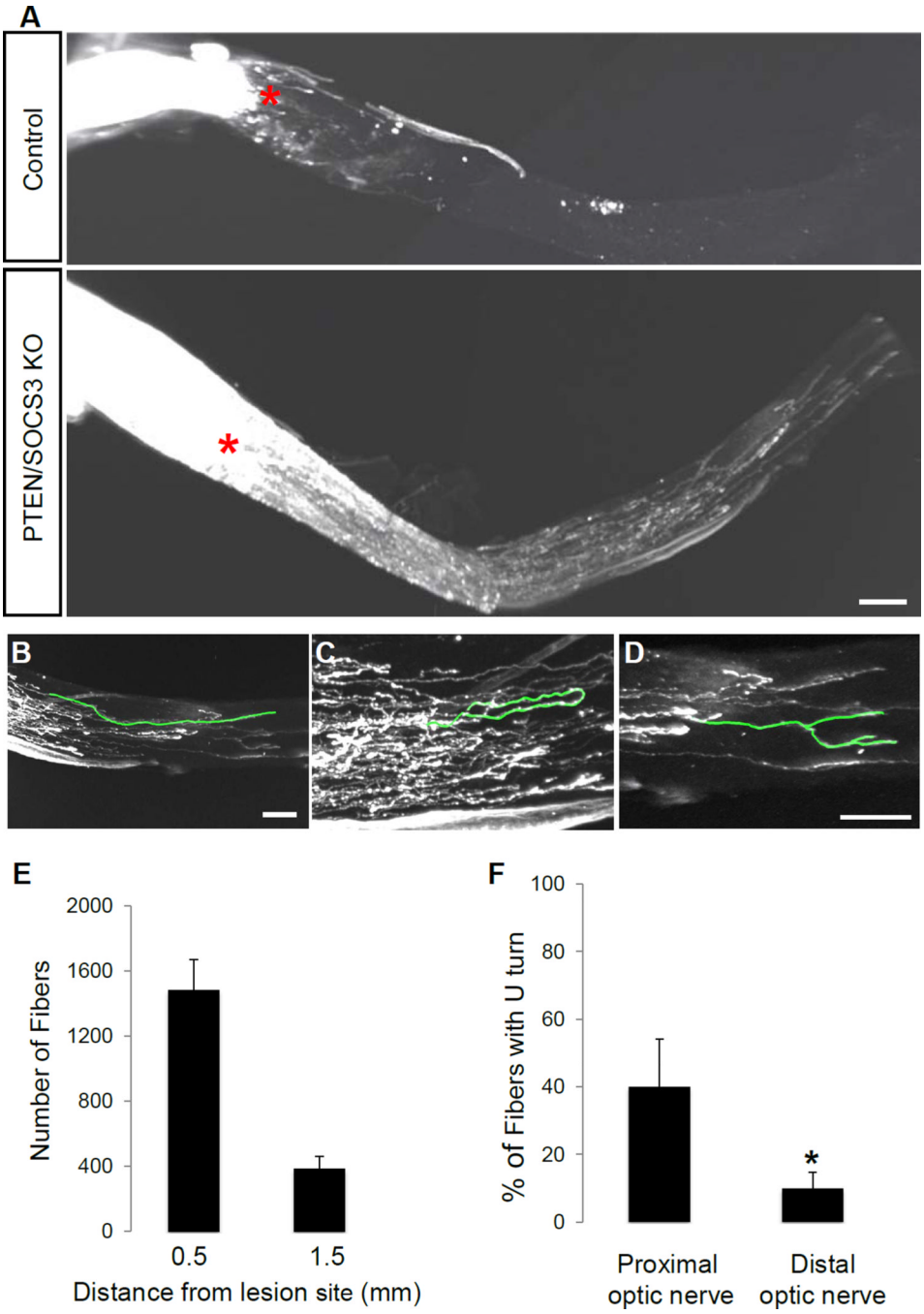

Figure 2.

3D assessment of regenerated RGC axons in the cleared optic nerve. **A**, 3D reconstructed optic nerves of control AAV-GFP treated mice and PTEN/SOCS3 KO mice at 17 days post-injury. **B–D**, neurite tracing of single fiber showing different growth patterns. Some axons travels in a relatively straight along the optic nerve towards the chiasm (to the right side of the image) as shown in **B**, or loop back towards the eye (to the left side of the image) as shown in **C**. Some axons generate branches as they extend within the optic nerve as shown in **D**. **E**, quantification of the number of CTB-labeled axons found at different distances

away from the lesion site (n=5). Red asterisk, lesion site. *p < 0.01, Student's t test. Scale bars, 200 μm.

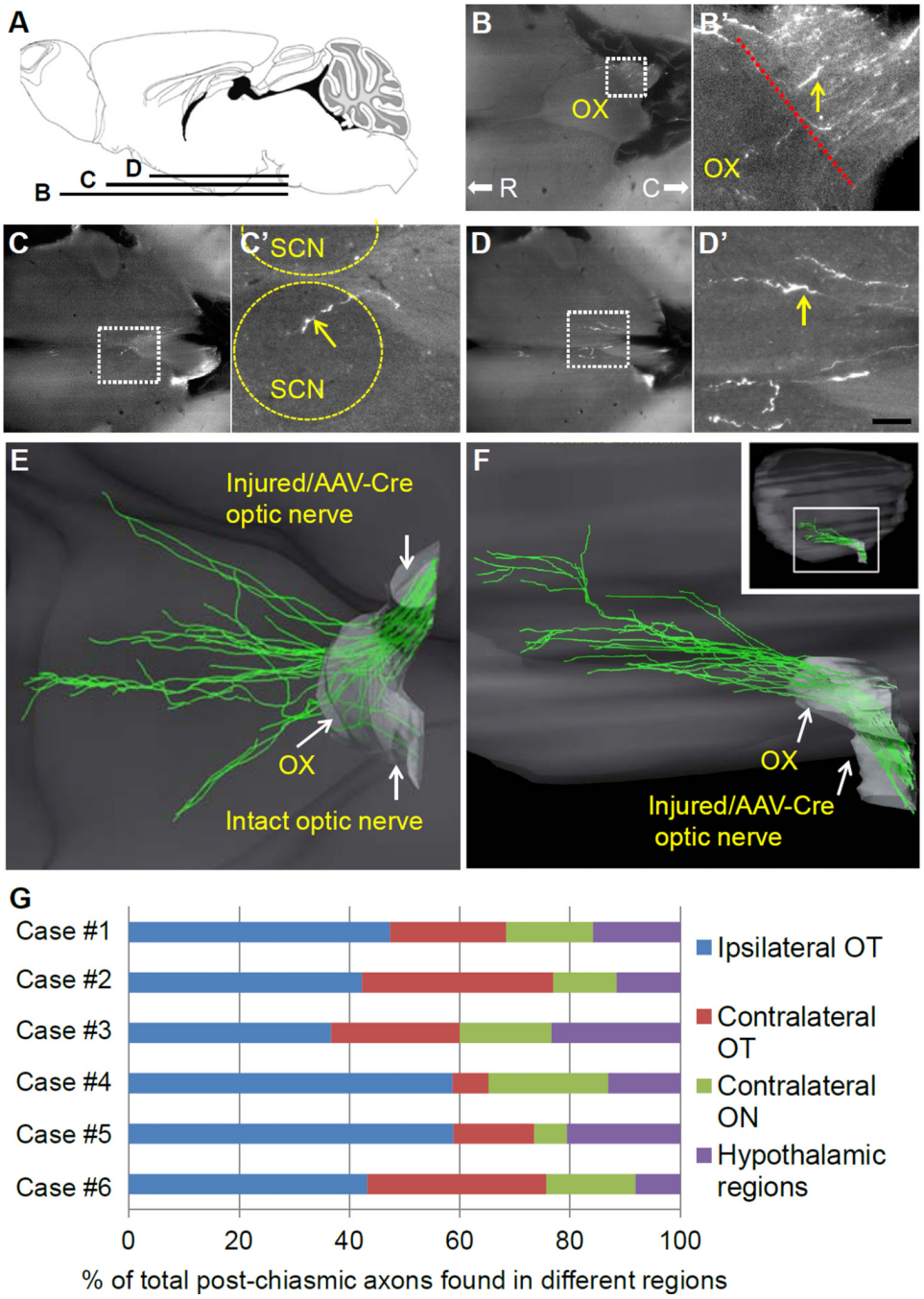

Figure 3.

3D visualization of axonal projections in the brain. **A**, schematic diagram of mouse brain showing horizontal planes at which individual optical slices in **B–D** are derived from. **B–D**, several representative horizontal optical slices collected from an unsectioned brain of PTEN/SOCS3 KO animal following LSFM. **B'– D'**, higher magnification of the respective white boxed area in **B–D**. Yellow arrows indicate CTB-labeled axons. CTB-labeled axons are found immediately before the optic chiasm as shown in **B**. Some axons extended medial-dorsally into the hypothalamic brain regions including the SCN as shown in **C**, and medial pre-optic area as shown in **D**. **E**, ventral view of the 3D reconstruction of traced fibers near

the optic chiasm. Neurite tracing and 3D volume rendering were done using Imaris software. **F**, lateral view of the 3D reconstruction of axonal projections into the brain. Inset shows low magnification of the whole brain following 3D reconstruction. **G**, quantification of axonal trajectory into different regions (i.e. ipsi/contralateral optic tracts, opposite optic nerve or hypothalamic regions). Values are presented as percentages of total axons that have exited the optic chiasm in 6 individual animals (case #1–6). C, caudal; ON, optic nerve; OT, optic tract; OX, optic chiasm; R, rostral; SCN, suprachiasmatic nucleus. Scale bar, 100 μm in **D**.

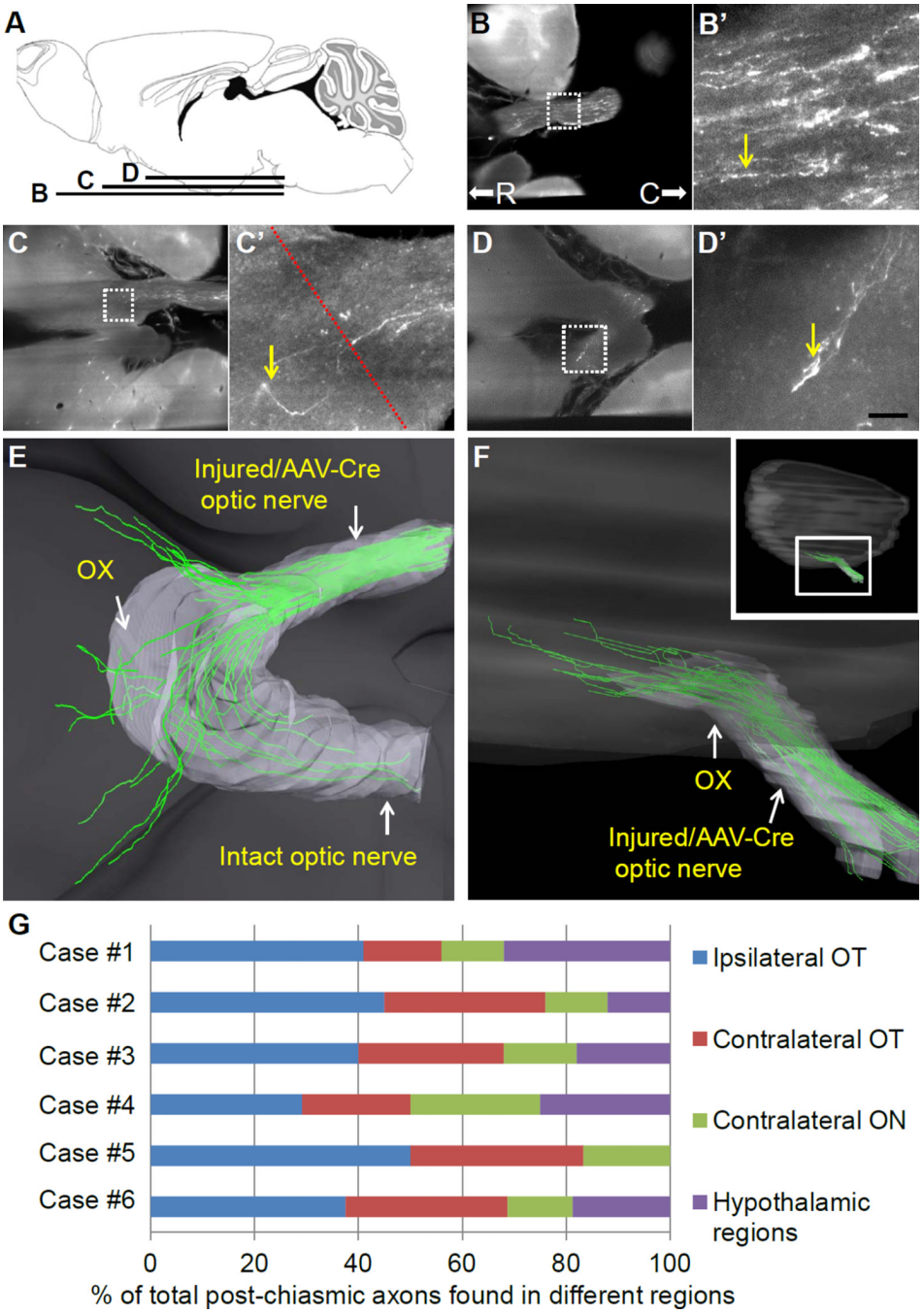

Figure 4.

3D visualization of axonal projections in the brain of PTEN KO/ZYM/cAMP mice. **A**, schematic diagram of mouse brain showing horizontal planes at which the images in **B–D** are derived from. **B–D**, several representative horizontal optical slices collected from an unsectioned brain of PTEN KO/ZYM/cAMP animal following LSFM. **B'– D'**, higher magnification of the respective white boxed area in **B–D**. Yellow arrows indicate CTB-labeled axons. CTB-labeled axons are found in the distal optic nerve near the optic chiasm as shown in **B**, in the SCN as shown in **C** and in the optic tract as shown in **D**. **E**, ventral view of the 3D reconstruction of traced fibers near the optic chiasm. **F**, lateral view of the

3D reconstruction of axonal projections into the brain. Inset shows low magnification of the whole brain following 3D reconstruction. **G**, quantification of axonal trajectory into different regions (i.e. ipsi/contralateral optic tracts, opposite optic nerve or hypothalamic regions). Values are presented as percentages of total axons that have exited the optic chiasm in 6 individual animals (case #1–6). Red dotted line in **C'** represents optic nerve-optic chiasm transition zone. C, caudal; ON, optic nerve; OT, optic tract; OX, optic chiasm; R, rostral; SCN, suprachiasmatic nucleus. Scale bar, 100 μm in **D**.

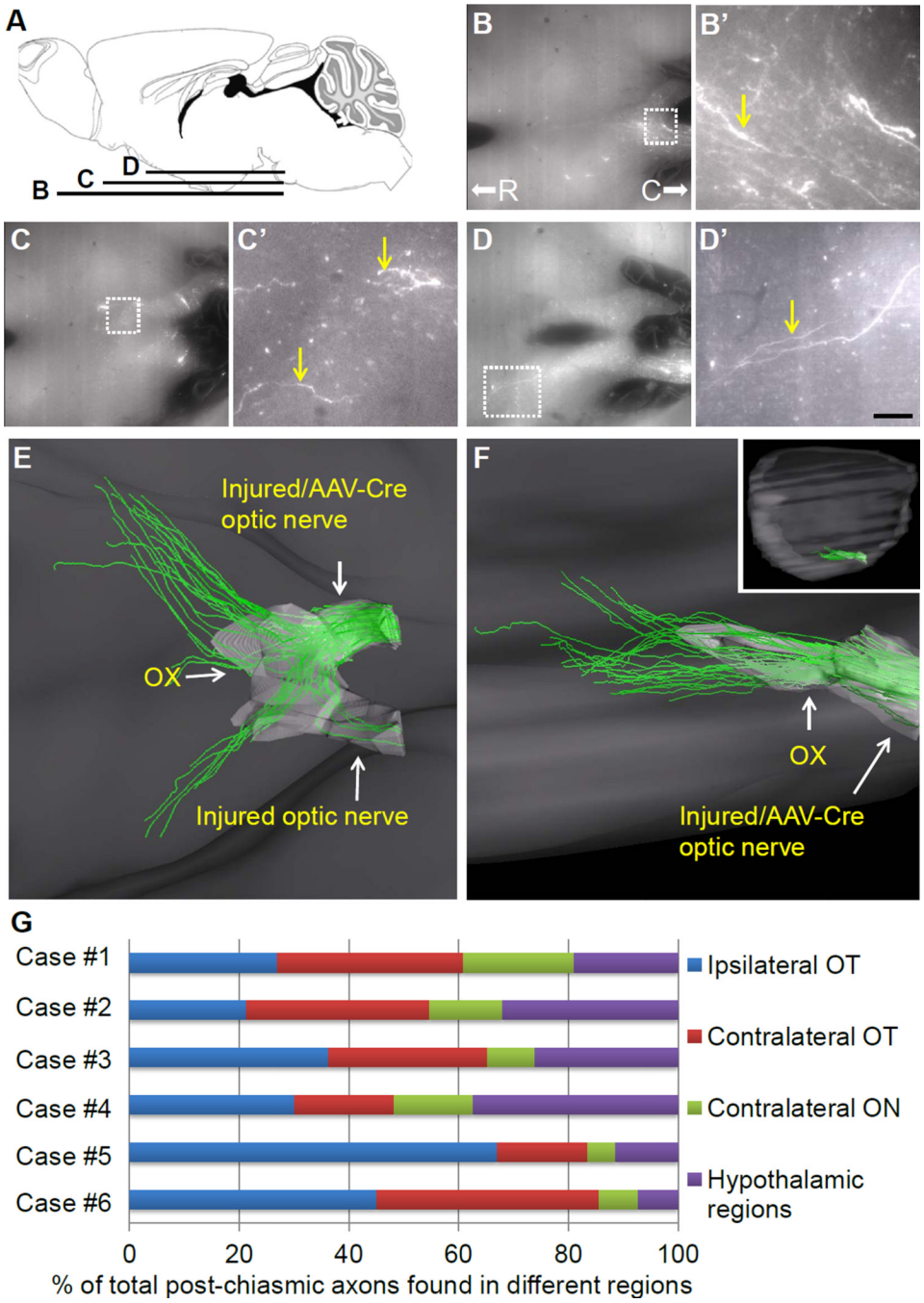

Figure 5.

3D visualization of axonal projections in the brain following bilateral optic nerve crush. **A**, schematic diagram of mouse brain showing horizontal planes at which the images in **B–D** are derived from. **B–F**, several representative horizontal optical slices collected from an unsectioned brain of PTEN/SOCS3 KO animal following LSFM. **B'–D'**, higher magnification of the respective white boxed area in **B–F**. Yellow arrows indicate CTB-labeled axons. CTB-labeled axons extend through the optic chiasm and into the optic tracts and hypothalamus. **E**, ventral view of the 3D reconstruction of traced fibers near the optic chiasm. **F**, lateral view of the 3D reconstruction of axonal projections into the brain. Inset

shows low magnification of the whole brain following 3D reconstruction. **G**, Quantification of axonal trajectory into different regions (i.e. ipsi/contralateral optic tracts, opposite optic nerve or hypothalamic regions). Values are presented as percentages of total axons that have exited the optic chiasm in 6 individual animals (case #1–6). C, caudal; ON, optic nerve; OT, optic tract; OX, optic chiasm; R, rostral; SCN, suprachiasmatic nucleus. Scale bar, 100 μm in **D**.